DISCUSSION OF NUMERICAL DEFICIENCY OF APPLYING A PARTIALLY WEIGHTED UPWIND FINITE-ELEMENT MODEL TO INCOMPRESSIBLE NAVIER-STOKES EQUATIONS

Tony W. H. Sheu, S. F. Tsai, and Morten M. T. Wang
Department of Naval Architecture and Ocean Engineering, National Taiwan University, 73 Chou-Shan Road, Taipei, Taiwan

The streamline upwind technique is extended to quadratic elements to analyze incompressible and viscous flow equations cast in the steady state. The biased part of the weighting functions is devised to achieve a nodally exact discretized one-dimensional equation, with an emphasis on grid nonuniformity. Two classes of upwinding finite-element models are considered. Our primary goal is to address the deficiency of the partially weighted finite-element model. Assessment is made of the stability and accuracy of the schemes devised. The integrity of the weighting functions chosen and the finite-element models considered is demonstrated analytically, and their performance is assessed systematically.

INTRODUCTION

Many engineering problems of practical relevance are concerned with incompressible Navier-Stokes equations. In the past, this class of flows was only experimentally tractable. Only recently has the advent of powerful computational environments and the rapidly declining cost-to-performance ratio of computer hardware made possible prediction of Navier-Stokes fluid flows [1]. Applied mathematicians and research engineers have turned to analyzing fluid engineering problems by solving the corresponding nonlinear initial-boundary-valued problems. Furthermore, thanks to continued advances in interactive pre- and postprocessing software, we can make use of computational fluid dynamics (CFD) techniques to explore complex flows and obtain new physical insight. Many industries are benefiting greatly from currently available computer programs that are dedicated to simulating incompressible viscous fluid flows in an arbitrary domain. Suffice it to say that the technique of CFD is emerging from research status and is becoming a way to investigate physical phenomena.

Despite several decades of numerical experience, conclusive numerical approximation of incompressible flow system is not yet fully at hand, even in the absence of a viscous effect [1]. Many obstacles still remain to obtaining highly accurate flow simulations. Some of the difficulties will be addressed in this article. Essential for simulation quality is assessment of accuracy, stability, disk storage, and ease of programming. As for incompressible Navier-Stokes equations, we face

Received 12 August 1996; accepted 19 March 1997.

Address correspondence to Professor Tony W. H. Sheu, Department of Naval Architecture and Ocean Engineering, National Taiwan University, 73 Chou-Shan Road, Taipei, Taiwan, Republic of China. E-mail: sheu@indy.na.ntu.edu.tw

Numerical Heat Transfer, Part B, 32:197–214, 1997

1040–7790/97 $12.00 + .00

NOMENCLATURE

a, b	constant-velocity vector field	δ	variable defined in Eq. (9)
c	rate of convergence defined in Eq. (17)	ν	kinematic viscosity
D_u, P_u	discretization errors	τ	intrinsic time scale
$\mathbf{f}$	source vector		
M^i	bilinear shape functions	**Subscripts**	
N^i	biquadratic shape functions		
p	pressure		
q	weighting function used in continuity equation	C	used for the fully weighted finite-element model
Re	Reynolds number	E	used for the partially upwinding finite-element model
$\mathbf{u}$	velocity vector		
$\mathbf{w}$ (or W^i)	weighting functions used in momentum equations	ref	indication of reference values
		s	streamline coordinate

the dilemma of having to reconcile solution accuracy and numerical stability. It is often the case that a gain in stability goes along with a loss in accuracy. For problems of the diffusion-dominant type, employment of a center-based discretization scheme can yield satisfactory results as a whole. Under these circumstances, spurious oscillations or wiggles, unfortunately, occur in the velocity solution when convection largely dominates diffusion [1]. While standard upwind schemes serve as a common cure for the enhancement of instabilities arising from convective terms, they are accompanied by a deterioration of accuracy. Such a drawback is attributable to grid lines that are out of alignment with the spatial flow directions. In reality, the transport phenomenon in the flow is simultaneously affected by the convection and diffusion effects. A discretization scheme capable of alleviating nonlinear oscillations, but not at the cost of obscuring the diffusion of the flow, is needed. We thus explore in depth here the issues involved in achieving high-order-accurate and nonoscillatory solutions to advection/diffusion problems.

In this article, we first present a closure problem for the target incompressible viscous fluid. A discretization method that is classified as a weighted residuals variant is employed as an analysis vehicle. Attention is focused on the implementation of upwind procedures on the pressure gradients and diffusive fluxes. This is followed by a derivation of the analytic weighting functions for two investigated finite-element models. For this study, modified equations are derived for each linearized governing equation. As is usual, analytic tests are carried out in this article not only for validation, but also for assessment purposes. Finally, we offer conclusions.

WORKING EQUATIONS AND THE FINITE-ELEMENT MODEL

The governing equations of incompressible and viscous fluid flows are cast in the following dimensionless form:

$$\nabla \cdot \mathbf{u} = 0 \tag{1}$$

$$\mathbf{u} \cdot \nabla \mathbf{u} + \nabla p - \frac{1}{\text{Re}} \nabla^2 \mathbf{u} = \mathbf{f} \tag{2}$$

In Eq. (2), $\mathrm{Re} \doteq U_{\mathrm{ref}} L_{\mathrm{ref}}/\nu$ stands for the Reynolds number, where L_{ref} is the characteristic length, U_{ref} is the reference velocity, ν is the kinematic viscosity, and $\mathbf{f}$ is the source term. Of applicable working variables, we advocate adopting the primitive-variable setting for use in the incompressible flow analysis. The main reason why we are in favor of this velocity-divergence form is rooted in the fact that the legitimate closure boundary condition is accessible [1]. In the notation of primitive variables, the elliptic partial differential equations (1)–(2) are subject only to boundary velocities. Specification of pressure conditions at the physical boundary will overdetermine the differential system [2].

Mixed and segregated formulations have emerged as being among the most popular classes of methods to solve equations (1)–(2). The mixed finite-element method has found some application in two-dimensional problems. An extension of this formulation to three-dimensional analyses suffers from ill-conditioning matrix equations. This presents obstacles to extending the application scope. Even so, the mixed formulation still outperforms its segregated counterpart because the kinematic constraint of a divergence-free vector field is unconditionally assured. We concentrate in this study on the coupled rather than the segregated formulation.

The variational statement characterizing the conservation equations (1)–(2) is as follows. For an admissive function $\mathbf{w} \in H_0^1(\Omega) \times H_0^1(\Omega)$ and a pressure mode $q \in L^2(\Omega)/\mathscr{R} = P$, find the weak solutions of velocity-pressure $(\mathbf{u}, p) \in V \equiv (H_0^1 \times H_0^1) \times P$ from the following equations:

$$\int_\Omega (\mathbf{u} \cdot \nabla \mathbf{u}) \cdot \mathbf{w}\, d\Omega + \frac{1}{\mathrm{Re}} \int_\Omega \nabla \mathbf{u} : \nabla \mathbf{w}\, d\Omega + \int_\Omega p \nabla \cdot \mathbf{w}\, d\Omega = \int_\Omega \mathbf{f} \cdot \mathbf{w}\, d\Omega \qquad \forall \mathbf{w} \in H \tag{3}$$

$$\int_\Omega (\nabla \cdot \mathbf{u}) q\, d\Omega = 0 \qquad \forall q \in P \tag{4}$$

Within the finite-element framework, we approximate primitive variables by virtue of the trial functions $M(\mathbf{x})$ for the pressure and $N(\mathbf{x})$ for the velocity vector. The key to suppressing oscillatory pressures lies in appropriate selection of the finite element. The guideline is that the finite element chosen must accommodate the inf-sup stability condition [3, 4]. Recognizing this, the shape functions for $N(\mathbf{x})$ and $M(\mathbf{x})$ are chosen as biquadratic and bilinear polynomials, respectively.

Depending on the degree of advection dominance, different finite-element models are recommended. In circumstances where physical diffusion largely dominates convection, the velocity direction has a negligible impact on the physics of flow. As a result, the Galerkin method is more advantageous. The Galerkin model, however, is prone to velocity oscillations for flows characterized by high Reynolds numbers [1]. In order to cope with numerical pathologies resulting from the prevailing convection, we place more emphasis on the upstream information in the hope of gaining a more stable discrete system. Upwind finite elements can be constructed in two ways. Among the different choices of adding upwinding to the formulation, we can refine the standard Galerkin method by adding artificial diffusions [5, 6] or by modifying the weighting functions to result in a Petrov-

Galerkin method [1]. In what follows, we refer to the first approach as a partially weighted model because the added diffusion to the Galerkin model corresponds to applying biased weighting functions only to convection terms.

Partially Weighted Finite-Element Model

In circumstances where the upstream information becomes increasingly important, employment of a Petrov-Galerkin finite element is essential to the convergence of solutions. By definition, biased weighting functions are equally applied to convective, diffusive, and pressure gradient terms to stabilize the discrete system. This poses difficulties of dealing with diffusive terms. As the elliptic nature of the diffusive and pressure gradient terms stands, we have the rational choice of applying the biased weighting solely to advection terms [5–9]. These terms add numerical stability to the Galerkin formulation without the expense of complicating the analysis in the treatment of second-order spatial derivatives in the equations. This model amounts to adding explicit artificial viscosities to the Galerkin finite-element method.

In support of the aforementioned statement, we will use a linearized x-momentum equation as an example. Given constant velocities a and b, the x-momentum equation is linearized as

$$au_x + bu_y + p_x - \frac{1}{\text{Re}}(u_{xx} + u_{yy}) - f_1 = 0 \tag{5}$$

Development of streamline upwind Petrov-Galerkin models to incompressible fluid flows has been mostly constructed under linear elements [10]. Comparatively few articles [11–14] have been dedicated to quadratic elements. For this study, our goal is to construct an analytic weighting function in quadratic elements.

The weighting functions are regarded as upwind modification of shape functions N_i. That is,

$$W^i = N^i + \tau N^j \tilde{V}_k^j \frac{\partial N^i}{\partial x_k} \tag{6}$$

where $\tilde{V}_k^j$ $(k = 1,2)$ are the linearized nodal velocities, and τ is the intrinsic time scale. By substituting shape functions for u and p, and the weighting function given above into the weighted residuals statement, the following modified equation is obtained:

$$au_x + bu_y + p_x - \frac{1}{\text{Re}}(u_{xx} + u_{yy}) - f_1 = \tau\left(a^2 u_{xx} + 2ab u_{xy} + b^2 u_{yy}\right) + D_u + P_u \tag{7}$$

The mathematical manipulation is, of course, considerable. Our attempt is to justify the use of chosen weighting functions can add a streamline artificial stabilization to the formulation. By taking into consideration the identity

$$a^2 u_{xx} + 2ab u_{xy} + b^2 u_{yy} = (a^2 + b^2) u_{ss}$$

the above equation can be rewritten as

$$au_x + bu_y + p_x - \frac{1}{\mathrm{Re}}(u_{xx} + u_{yy}) - f_1 = \tau(a^2 + b^2)u_{ss} + D_u + P_u \tag{8}$$

where s denotes the local flow direction. Clearly revealed from Eq. (8) is the introduction of stabilization, as seen from the first term on the right-hand side of Eq. (8), to the original Eq. (5). This modified equation analysis helps to reveal that an application of biased weighting functions to advection terms corresponds to implicitly adding an artificial viscosity with positive sign to the Galerkin framework. While this strategy causes the stability to enhance, this scheme also encounters some ambiguity in consistency. We will study this issue analytically and numerically in the remaining sections.

It remains to determine τ in Eq. (6), which is responsible for the degree of upwinding and is thus of great consequence. To this end, the derivation of τ proceeds along the line of equating the nodal finite-element solutions with the exact solution. In quadratic elements, we can divide velocity nodal points into two groups, end and center nodes. While the expression for τ is analytically feasible in one dimension, extension to multidimensional analysis is quite involved and is often insuperable. Our strategy for the development of the streamline upwinding model is to keep the formulation analytic in one dimension. Within the one-dimensional context, we make use of the operator-splitting approximation to yield the following expression for τ:

$$\tau = \frac{\delta(\gamma_\xi)V_\xi h_\xi + \delta(\gamma_\eta)V_\eta h_\eta}{2|V|^2} \tag{9}$$

where $\gamma_\xi = V_\xi h_\xi \,\mathrm{Re}/2$, $\gamma_\eta = V_\eta \,\mathrm{Re}/2$, $V_\xi = \hat{\mathbf{e}}_\xi \cdot V$, and $V_\eta = \hat{\mathbf{e}}_\eta \cdot V$. Here $\hat{\mathbf{e}}_\xi$ and $\hat{\mathbf{e}}_\eta$ are the local coordinate basis unit vectors.

We now turn to determining $\delta_E(\gamma_\xi)$ from the one-dimensional scalar convection-diffusion equation. In a nonuniformly discretized quadratic element, as shown in Figure 1, the analytic expressions for $\delta_E(\gamma_\xi)$ vary with the local Peclet number in

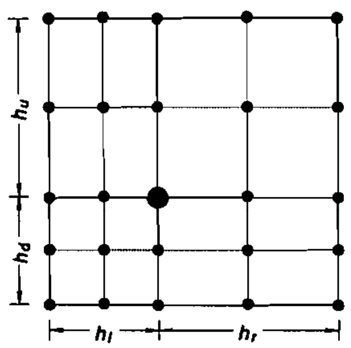

Figure 1. Illustration of nonuniform grid discretization for a point marked by ●.

the following way:

$$\delta_E(\gamma_\xi) = \begin{cases} \alpha_E(h_{rl}, \gamma_l) & \text{at end nodes} \\ \beta(\gamma) & \text{at center nodes} \end{cases} \tag{10}$$

where

$$\alpha_E(h_{rl}, \gamma_l) = \frac{\begin{array}{r} -(h_{rl} + h_{rl}\gamma_l)e^{-2\gamma_l} + 4(2h_{rl} + h_{rl}\gamma_l)e^{-\gamma_l} - 7(h_{rl} + 1) \\ +4(2 - h_{rl}\gamma_l)e^{h_{rl}\gamma_l} - (1 - h_{rl}\gamma_l)e^{2h_{rl}\gamma_l} \end{array}}{h_{rl}\gamma_l(e^{-2\gamma_l} - 8e^{-\gamma_l} + 14 - 8e^{h_{rl}\gamma_l} + e^{2h_{rl}\gamma_l})}$$

$$\beta = \frac{1}{2}\coth\left(\frac{\gamma}{2}\right) - \frac{1}{\gamma}$$

$$h_{rl} = \frac{h_r}{h_l}$$

$$\gamma_l = \frac{u_e h_l \,\mathrm{Re}}{2}$$

$$\gamma = \frac{u_c h \mathrm{Re}}{2}$$

To give readers a picture of how δ_E varies with the cell Reynolds number in a nonuniform element, we first define u_e and u_c in Figure 2 and then plot δ_E. It is

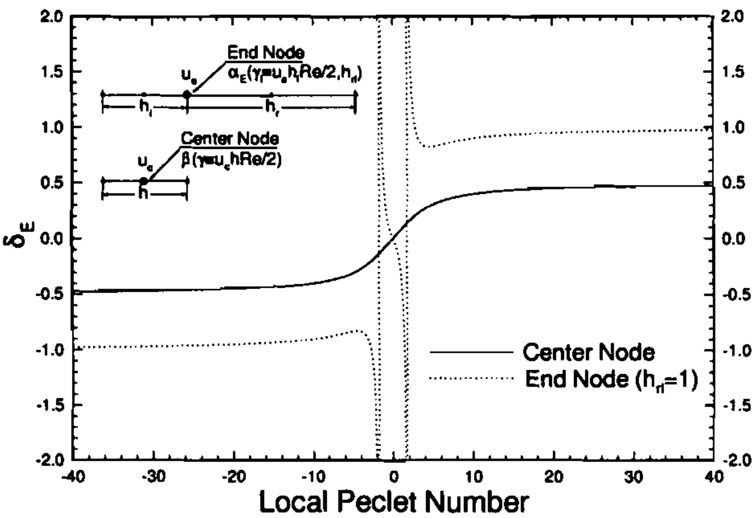

Figure 2. Illustration of $\delta_E(\gamma)$, as defined in Eq. (10), against the local Peclet number γ.

noticeable that the values of δ_E are not necessarily positive. It is this physically irrelevant, artificial viscosity that accounts for the divergent solutions in this analysis. To cope with this difficulty, it is recommended that α_E be replaced with β in the subsequent analysis for purposes of comparison.

Fully Weighted Finite-Element Model

Upwinding is essential to obtain converged solutions for high-Reynolds-number cases encountered in the incompressible Navier-Stokes flow simulation. We adopt the Petrov-Galerkin method, where the test functions **w** are regarded as the upwind-weighted refinements to the basis functions N. While the discrete system is enhanced, the solution accuracy deteriorates as a result of this biased addition. In cases where grid lines are out of alignment with flow directions, the computed solutions may be seriously contaminated and the real physics thus obscured. This type of prediction inaccuracy is the so-called false diffusion error [15, 16]. To avoid this commonly encountered problem, we resort to adopting a flow-oriented upwind model. The streamline upwind technique previously developed for linear elements is particularly effective in enhancing stability along the flow direction and is extended here to quadratic elements. The aim is to gain higher accuracy and, at the same time, to stabilize the calculations at high Reynolds numbers. In what follows, we will assign the biased weighting functions as defined in Eqs. (6) and (9) to retain the streamline upwinding character.

By substituting these interpolation equations into Eqs. (3–4), together with use of weighting functions given in Eq. (6), we can derive the following unsymmetric matrix equations:

$$\left[\int_{\Omega^h}\begin{Bmatrix} C^{ij} & 0 & -M^j \dfrac{\partial N^i}{\partial X_1} + B^i \dfrac{\partial M^j}{\partial X_1} \\ 0 & C^{ij} & -M^j \dfrac{\partial N^i}{\partial X_2} + B^i \dfrac{\partial M^j}{\partial X_2} \\ M^i \dfrac{\partial N^j}{\partial X_1} & M^i \dfrac{\partial N^j}{\partial X_2} & 0 \end{Bmatrix} d\Omega^h\right]\begin{pmatrix} u_j \\ v_j \\ p_j \end{pmatrix} = \mathbf{0} \qquad (11)$$

where

$$\begin{aligned} C^{ij} &= (N^i + B^i)\left(N^j \tilde{V}_k^j\right)\frac{\partial N^j}{\partial x_k} + \frac{1}{\text{Re}}\frac{\partial N^i}{\partial x_k}\frac{\partial N^j}{\partial x_k} - \frac{1}{\text{Re}} B^i \frac{\partial^2 N^j}{\partial x_k\,\partial x_k} \\ B^i &= \tau_c N^j \tilde{V}_k^j \frac{\partial N^i}{\partial x_k} \end{aligned} \qquad (12)$$

Before solving the resulting indefinite and unsymmetric matrix equations by using a frontal direct solver, the expression of δ in Eq. (9) is required. In a nonuniformly discretized quadratic element, we implement upwinding approximation on each term shown in the one-dimensional convection-diffusion equation. The analytic expression of δ_C is thus derived as follows:

$$\delta_C(\gamma_\xi) = \begin{cases} \alpha_C(h_{rl}, \gamma_l) & \text{at end nodes} \\ \beta(\gamma) & \text{at center nodes} \end{cases} \tag{13}$$

where

$$\alpha_C(h_{rl}, \gamma_l) = \frac{\begin{array}{r} -(h_{rl} + h_{rl}\gamma_l)e^{-2\gamma_l} + 4(2h_{rl} + h_{rl}\gamma_l)e^{-\gamma_l} - 7(h_{rl} + 1) \\ +4(2 - h_{rl}\gamma_l)e^{h_{rl}\gamma_l} - (1 - h_{rl}\gamma_l)e^{2h_{rl}\gamma_l} \end{array}}{\begin{array}{r} -(6h_{rl} - h_{rl}\gamma_l)e^{-2\gamma_l} + 4(3h_{rl} - 2h_{rl}\gamma_l)e^{-\gamma_l} + 14h_{rl}\gamma_l \\ +6(-h_{rl} + 1) - 4(3 + 2h_{rl}\gamma_l)e^{h_{rl}\gamma_l} + (6 + h_{rl}\gamma_l)e^{2h_{rl}\gamma_l} \end{array}}$$

$$\beta = \frac{1}{2}\coth\left(\frac{\gamma}{2}\right) - \frac{1}{\gamma}$$

$$h_{rl} = \frac{h_r}{h_l}$$

$$\gamma_l = \frac{u_e h_l \operatorname{Re}}{2}$$

$$\gamma = \frac{u_c h \operatorname{Re}}{2}$$

For the sake of completeness, we also plot δ_C against the Peclet numbers. In the limiting case of a uniform grid, the expression of δ_C, as shown in Figure 3, turns out to be that of Donea [13]:

$$\delta_D(\gamma) = \begin{cases} \alpha_D(\gamma) = \dfrac{2 - \cosh(\gamma) - (4/\gamma)\tanh(\gamma/2) + (1/\gamma)\sinh(\gamma)}{4\tanh(\gamma/2) - \sinh(\gamma) - (6/\gamma)\sinh(\gamma)\tanh(\gamma/2)} \\ \quad \text{at end nodes} \\ \beta(\gamma) = \frac{1}{2}\coth\left(\dfrac{\gamma}{2}\right) - \dfrac{1}{\gamma} \\ \quad \text{at center nodes} \end{cases} \tag{14}$$

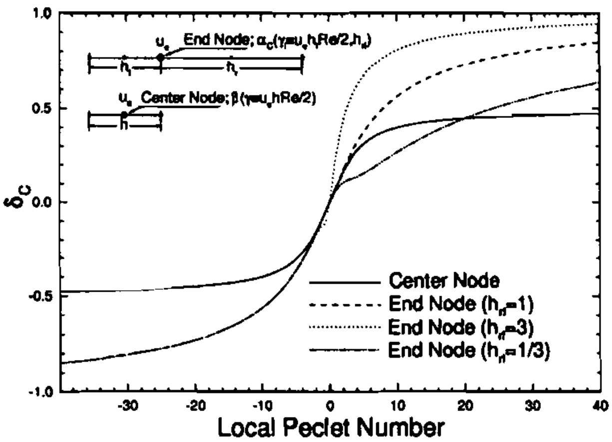

Figure 3. Illustration of $\delta_C(\gamma)$, as defined in Eq. (13), against the local Peclet number γ.

FUNDAMENTAL STUDIES ON THE DISCRETIZATION SCHEME

Modified Equations for Continuity and Momentum Equations

To gain additional details about two investigated finite-element models developed to solve incompressible Navier-Stokes equations, it is instructive to conduct a fundamental study in a domain of biquadratic elements. To begin with, we make a distinction between the differential equation and its discrete counterparts by conducting a Taylor series expansion for each discrete term. In the course of conducting this modified equation analysis, algebraic manipulation is considerable. Thanks to MAPLE [17], we can handle the algebraic complexities. Following the standard procedures of conducting the modified equation analysis, we can derive the following modified continuity equation:

$$u_x + v_y = -\left(\frac{h^2}{3}u_{xxx} + \frac{h^2}{3}u_{xyy} + \frac{h^4}{20}u_{xxxxx} + \frac{h^4}{9}u_{xxxyy} + \frac{h^4}{36}u_{xyyyy}\right)$$
$$-\left(\frac{h^2}{3}v_{xxy} + \frac{h^2}{3}v_{yyy} + \frac{h^4}{20}v_{xxxxy} + \frac{h^4}{9}v_{xxyyy} + \frac{h^4}{36}v_{yyyyy}\right) + \mathcal{O}(h^6) \tag{15}$$

The attainable scheme consistency is manifested by the discretization errors, shown on the right-hand side of Eq. (15), which approach zero divergence with an order of $\mathcal{O}(h^2)$.

We also perform Taylor series expansion on the linearized momentum equations. Due to space considerations, we only summarize the resulting modified

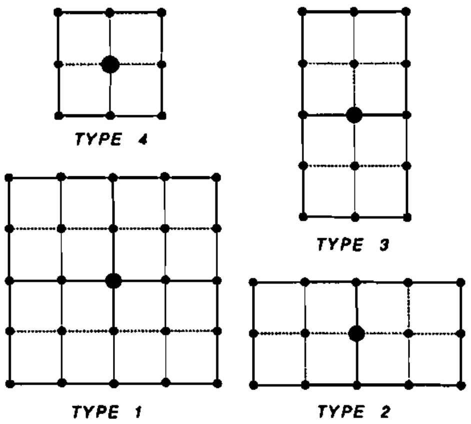

Figure 4. Four types of elements encountered in the derivation of modified equations for the finite-element model formulated in biquadratic elements.

equations. At four representative nodes, as marked by • in Figure 4, the modified equations for the x- and y-momentum equations take the following forms, respectively:

$$au_x + bu_y + p_x - \frac{1}{\mathrm{Re}}(u_{xx} + u_{yy}) - f_1 = (a^2 + b^2)\tau u_{ss} + D_u + P_u \qquad (8)$$

$$av_x + bv_y + p_y - \frac{1}{\mathrm{Re}}(v_{xx} + v_{yy}) - f_2 = (a^2 + b^2)\tau v_{ss} + D_v + P_v \qquad (16)$$

The discretization errors for the flux terms, D_u, D_v, and pressure gradients, P_u, P_v, are summarized in Tables 1 and 2, respectively. The intrinsic time scale τ takes the order of $\mathcal{O}(h/|\mathbf{u}|)$ in the advection-dominated case, and the order of $\mathcal{O}(\mathrm{Re}\, h^2)$ in the diffusion-dominated case.

According to the discretization terms summarized in Tables 1 and 2, the order of the method is $\mathcal{O}(h)$ in the advection-dominated case and $\mathcal{O}(h^2)$ in the diffusion-dominated case. As Eqs. (8) and (16) reveal, the damping terms are applied mainly to the flow direction. Physically relevant solutions are thus expected only when the value of τ is positive. With this favorable stability, computed finite-element solutions u and v do not grow with iterations.

COMPUTED RESULTS

As a first step in assessing simulation quality, we will consider a problem amenable to analytic solution. For problems whose solutions are classified as smooth, a good estimate of solution accuracy can be obtained using the L_2 error norm ($\|\cdot\|$). Whether or not the stability property is attainable depends indirectly on the rate of convergence, c, based on the finite-element solutions rendered at

Table 1. Discretization errors D_i $(i = u, v)$, as shown in Eqs. (8) and (16), for four types of elements in Figure 4

Coefficient element type	u_{xxx} or v_{xxx}	u_{xxy} or v_{xxy}	u_{xyy} or v_{xyy}	u_{yyy} or v_{yyy}
(*a*) Fully weighted model				
Type 1	$\frac{1}{3}\frac{a(-9\tau + h^2\,\mathrm{Re})}{\mathrm{Re}}$	$\frac{1}{5}\frac{b(-5\tau + h^2\,\mathrm{Re})}{\mathrm{Re}}$	$\frac{1}{5}\frac{a(-5\tau + h^2\,\mathrm{Re})}{\mathrm{Re}}$	$\frac{1}{3}\frac{b(-9\tau + h^2\,\mathrm{Re})}{\mathrm{Re}}$
Type 2	$\frac{1}{3}\frac{a(-9\tau + h^2\,\mathrm{Re})}{\mathrm{Re}}$	$\frac{1}{5}\frac{b(-5\tau + h^2\,\mathrm{Re})}{\mathrm{Re}}$	$-\frac{1}{10}\frac{a(10\tau + h^2\,\mathrm{Re})}{\mathrm{Re}}$	$-\frac{1}{6}bh^2$
Type 3	$-\frac{1}{6}ah^2$	$-\frac{1}{10}\frac{b(10\tau + h^2\,\mathrm{Re})}{\mathrm{Re}}$	$\frac{1}{5}\frac{a(-5\tau + h^2\,\mathrm{Re})}{\mathrm{Re}}$	$\frac{1}{3}\frac{b(-9\tau + h^2\,\mathrm{Re})}{\mathrm{Re}}$
Type 4	$-\frac{1}{6}ah^2$	$-\frac{1}{10}\frac{b(10\tau + h^2\,\mathrm{Re})}{\mathrm{Re}}$	$-\frac{1}{10}\frac{a(10\tau + h^2\,\mathrm{Re})}{\mathrm{Re}}$	$-\frac{1}{6}bh^2$
(*b*) Partially weighted model				
Type 1	$\frac{1}{3}ah^2$	$\frac{1}{5}bh^2$	$\frac{1}{5}ah^2$	$\frac{1}{3}bh^2$
Type 2	$\frac{1}{3}ah^2$	$\frac{1}{5}bh^2$	$-\frac{1}{10}ah^2$	$-\frac{1}{6}bh^2$
Type 3	$-\frac{1}{6}ah^2$	$-\frac{1}{10}bh^2$	$\frac{1}{5}ah^2$	$\frac{1}{3}bh^2$
Type 4	$-\frac{1}{6}ah^2$	$-\frac{1}{10}bh^2$	$-\frac{1}{10}ah^2$	$-\frac{1}{6}bh^2$

two consecutive grid systems of the spacings h_1 and h_2:

$$c = \frac{\ln \|e_1\| - \ln \|e_2\|}{\ln |h_1| - \ln |h_2|} \tag{17}$$

Test Problem 1

To begin, we consider a problem that is amenable to analytic solutions. For this problem, a square domain of unit length is covered with nonuniform grids, as shown in Figures 5*a* and 6*a*. The analytic pressure takes the form

$$p = \frac{-2}{(1 + x)^2 + (1 + y)^2} \tag{18}$$

Table 2. Discretization errors P_i ($i = u, v$), as shown in Eqs. (8) and (16), for four types of elements, as given in Figure 4, using the fully-weighted finite-element model

	P_{xx}	P_{xy}	P_{yy}	P_{xxx}	P_{xxy}	P_{xyy}	P_{yyy}
(*a*) *x*-Momentum equation							
Type 1	$3\tau a$	τb	0	$-\frac{2}{3}h^2$	0	0	0
Type 2	$3\tau a$	τb	0	$-\frac{2}{3}h^2$	0	$-\frac{1}{2}h^2$	0
Type 3	0	τb	0	$-\frac{1}{6}h^2$	0	0	0
Type 4	0	τb	0	$-\frac{1}{6}h^2$	0	$-\frac{1}{2}h^2$	0
(*b*) *y*-Momentum equation							
Type 1	0	τa	$3\tau b$	0	0	0	$-\frac{2}{3}h^2$
Type 2	0	τa	0	0	0	0	$-\frac{1}{6}h^2$
Type 3	0	τa	$3\tau b$	0	$-\frac{1}{2}h^2$	0	$-\frac{2}{3}h^2$
Type 4	0	τa	0	0	$-\frac{1}{2}h^2$	0	$-\frac{1}{6}h^2$

on condition that the boundary velocities are specified analytically as follows:

$$u = \frac{-2(1+y)}{(1+x)^2 + (1+y)^2} \tag{19}$$

$$v = \frac{2(1+x)}{(1+x)^2 + (1+y)^2} \tag{20}$$

While the flow pattern defined by Eqs. (18)–(20) is quite smooth and simple, this problem is well suited to elucidating the deficiency that a discretization method may have. The underlying philosophy behind this argument is as follows: If use of a discretization scheme yields inaccurate solutions for a simple problem, then there must be plenty of room for further improvement.

While the above artificial-viscosity finite-element model retains the consistency property, erroneous pressures are clearly visible in Figures 5*b* and 6*b*. According to Tables 3 and 4, which tabulate the L_2 error norms, one order of deterioration of the rate of convergence is attributable to the Galerkin approximation of pressure gradient and diffusive terms.

The wiggles present in regions with graded nodes can be mostly suppressed by applying the biased weighting functions to the pressure gradient term. Improved

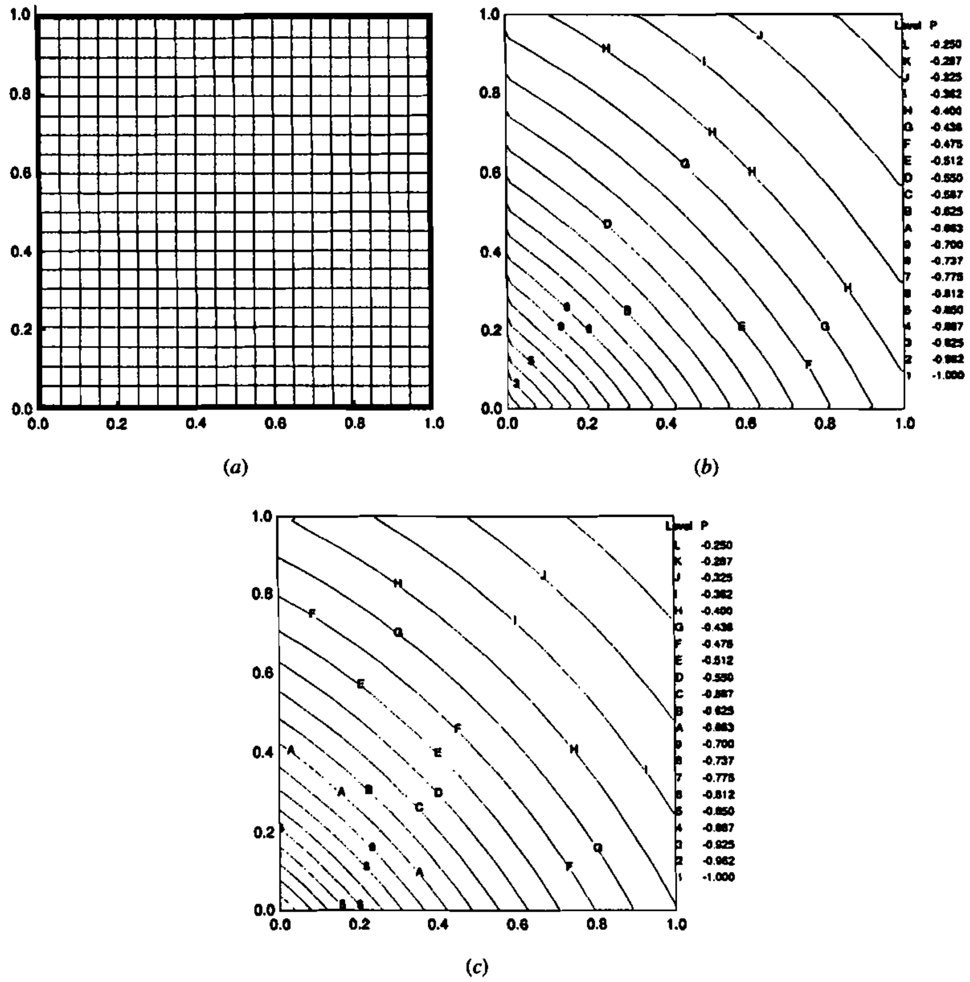

Figure 5. Grids and pressure contour plots: (*a*) nonuniform grids used in test problem 1; (*b*) computed pressure contours based on the partially weighted finite-element model; (*c*) computed pressure contours based on a finite-element model where pressure gradient terms are unsymmetrically weighted.

stability is manifested in Figures 5*c* and 6*c*. In summary, this test problem demonstrates the rational use of the fully weighted finite-element model instead of the partially weighted finite-element model.

Test Problem 2

A more stringent test problem will be considered to elucidate the deficiency of applying Galerkin approximation to diffusive fluxes. This problem is known as the Kovasznay flow problem [18]. This benchmark problem is also amenable to the

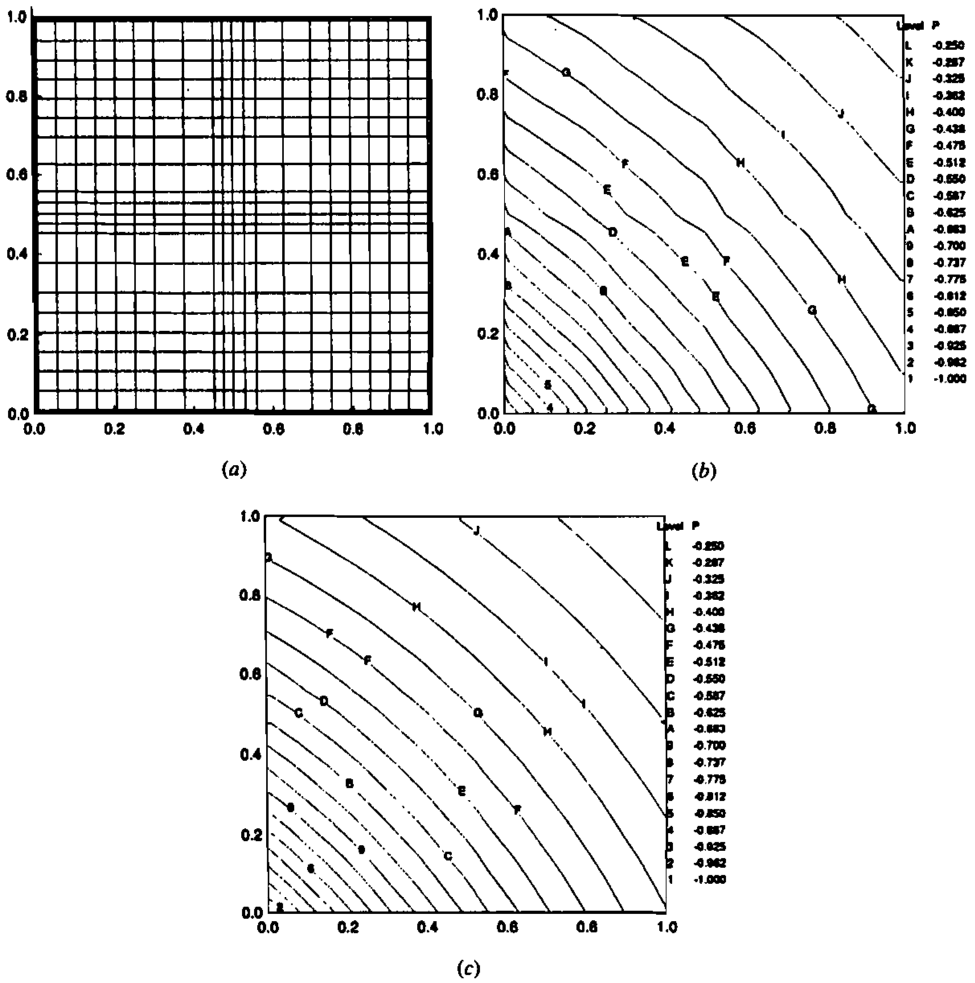

Figure 6. Grids and pressure contour plots: (*a*) nonuniform grids used in test problem 1; (*b*) computed pressure contours based on the partially weighted finite-element models; (*c*) computed pressure contours based on a finite-element model where pressure gradient terms are unsymmetrically weighted.

Table 3. Computed L_2 error norms and convergent orders using the partially weighted finite-element model

Mesh size	$\|\mathbf{u} - \mathbf{u}_{exact}\|$	Convergent order	$\|p - p_{exact}\|$	Convergent order
10 × 10	3.184×10^{-4}		1.244×10^{-3}	
20 × 20	1.634×10^{-4}	0.962	5.093×10^{-4}	1.288

Table 4. Computed L_2 error norms and convergent orders using the fully-weighted finite-element model

Mesh size	$\|\mathbf{u} - \mathbf{u}_{exact}\|$	Convergent order	$\|p - p_{exact}\|$	Convergent order
10 × 10	3.757×10^{-4}		6.086×10^{-4}	
20 × 20	8.187×10^{-5}	2.091	1.421×10^{-4}	2.099

analytic solution given by

$$u = 1 - e^{\lambda x}\cos(2\pi y) \tag{21}$$

$$v = \frac{\lambda}{2\pi} e^{\lambda x}\sin(2\pi y) \tag{22}$$

$$p = \frac{1}{2}(1 - e^{2\lambda x}) \tag{23}$$

Here, the value of λ takes $\lambda = (\mathrm{Re}/2) - [(\mathrm{Re}^2/4) + 4\pi^2]^{1/2}$.

Performing a biased weighting on the diffusive fluxes presents numerical difficulty in manipulating the second-order spatial derivatives, one of which is

$$\frac{\partial^2 N}{\partial x_i^2} = \frac{\partial N}{\partial \chi_j}\frac{\partial^2 \chi_j}{\partial x_i^2} + \frac{\partial^2 N}{\partial \chi_j \partial \chi_k}\frac{\partial \chi_j}{\partial x_i}\frac{\partial \chi_k}{\partial x_i} \qquad (i, j, k = 1, 2) \tag{24}$$

Here x_i $(i = 1, 2)$ denote the global coordinates, x, y, and χ_i $(i = 1, 2)$ denote the local coordinates (ξ, η). While the mathematic manipulation is considerable, implementation of the biased upwinding procedure on the diffusive terms is also important because it yields a more stable system. To justify our viewpoint, we have done numerical calculations in a square that is nonuniformly discretized only along the x direction. For test Reynolds numbers 100 and 1,000, the computed pressure profiles vary with y even though the velocity field is well predicted. This erroneous pressure is the apparent result of the omission of the biased weighting on the physical fluxes as seen in Figure 7, which depicts the computed y-independent pressures underlying the fully weighted finite-element model.

CONCLUSIONS

The main thrust of this work has been the evaluation of the potential for using upwind finite-element models to simulate steady, incompressible Navier-Stokes equations. These finite-element models can be classified into two main groups, the partially weighted and fully weighted upwind finite-element models. In the partially weighted finite-element context, we can further divide them into the

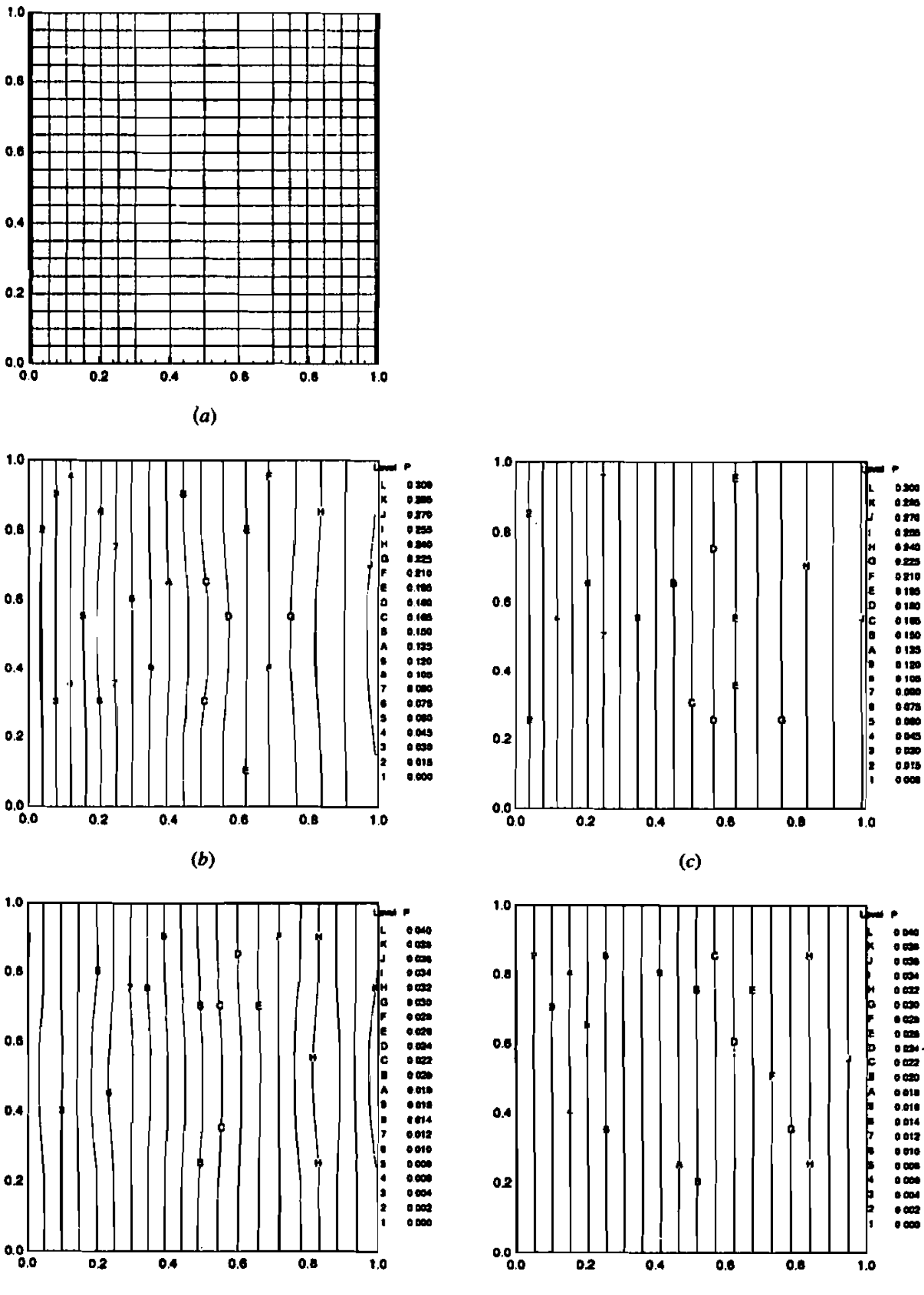

Figure 7. Computed pressure contours for test problem 2; (*a*) nonuniform grids; (*b*) Galerkin approximation on viscous fluxes for Re = 100; (*c*) fully weighted Petrov-Galerkin finite-element model for Re = 100; (*d*) Galerkin approximation on viscous fluxes for Re = 1,000; (*e*) fully weighted Petrov-Galerkin finite-element model for Re = 1,000.

one referred to as the artificial viscosity model and one that has been weighted, with a bias toward the upwind side, on the advective and the pressure gradient terms. The results obtained for the steady-flow case have been compared analytically among these models, and the results have indicated the fully weighted upwinding finite-element model's capability of predicting oscillation-free solutions in regions with clustered grids. The proposed models fall into the streamline upwind finite-element context and have been extended to quadratic elements, with an emphasis on grid nonuniformity. The model is upwind-weighted in the sense that it is algebraically analytic in a one-dimensional context. Discussion of the upwind finite-element models presented here has centered on modified equation analyses. This has provided useful insight into the fundamental issues of the scheme and the mathematics behind the solutions.

REFERENCES

1. M. D. Gunsburger, *Finite Element Methods for Viscous Incompressible Flows, A Guide to Theory, Practice, and Algorithms*, Academic Press, New York, 1989.
2. O. Ladyzhenskaya, *The Mathematical Theory of Viscous Incompressible Flow*, Gordon & Breach, New York, 1969.
3. F. Brezzi, On the Existence, Uniqueness and Approximation of Saddle Point Problems Arising from Lagrangian Multipliers, *RAIRO, Anal. Num.*, vol. 8, no. R2, pp. 129–151, 1974.
4. I. Babuška, Error Bounds for Finite Element Methods, *Numer. Math.*, vol. 16, pp. 322–333, 1971.
5. Z. Qin and M. D. Olson, Finite Element-Algebraic Closure Analysis of Turbulent Separated-Reattaching Flow around a Rectangular Body, *Comput. Meth. Appl. Mech. Eng.*, vol. 85, pp. 131–150, 1991.
6. Z. Qin and M. D. Olson, Finite Element-Algebraic Closure Modelling of Turbulent Separated Flow over a Backward-Facing Step: Steady and Unsteady Aspects, *Int. J. Numer. Meth. Heat Fluid Flow*, vol. 2, pp. 3–20, 1992.
7. J. G. Rice and R. J. Schnipke, An Equal-Order Velocity-Pressure Formulation That Does Not Exhibit Spurious Pressure Modes, *Comput. Meth. Appl. Mech. Eng.*, vol. 58, pp. 135–149, 1986.
8. T. E. Tezduyar, S. Mittal, and R. Shih, Time-Accurate Incompressible Flow Computations with Quadrilateral Velocity-Pressure Elements, *Comput. Meth. Appl. Mech. Eng.*, vol. 87, pp. 363–384, 1991.
9. C. T. Shaw, Using a Segregated Finite Element Scheme to Solve the Incompressible Navier-Stokes Equations, *Int. J. Numer. Meth. Fluids*, vol. 12, pp. 81–92, 1991.
10. A. N. Brooks and T. J. R. Hughes, Streamline Upwind Petrov-Galerkin Formulations for Convection Dominated Flows with Particular Emphasis on the Incompressible Navier-Stokes Equations, *Comput. Meth. Appl. Mech. Eng.*, vol. 32, pp. 199–259, 1982.
11. I. Christie and A. R. Mitchell, Upwinding of High Order Galerkin Methods in Conduction-Convection Problem, *Int. J. Numer. Meth. Eng.*, vol. 14, pp. 1764–1771, 1978.
12. J. C. Heinrich, On Quadratic Elements in Finite Element Solutions of Steady-State Convection-Diffusion Equations, *Int. J. Numer. Meth. Eng.*, vol. 15, pp. 1041–1052, 1980.
13. J. Donea, T. Belytschko, and P. Smolinski, A Generalized Galerkin Method for Steady Convection-Diffusion Problems with Application to Quadratic Shape Function Elements, *Comput. Meth. Appl. Mech. Eng.*, vol. 48, pp. 25–43, 1985.